A STUDY OF MULTI-DIMENSIONAL DRUG DIFFUSION IN MATRICES AND MEMBRANES

Achim Göpferich[1], Karlhans Endlich[2] and Geoffrey Lee[1],*

*[1]Institute for Pharmaceutical Technology and Biopharmaceutics, and [2]Department of Physics, Heidelberg University, INF 366, 6900 Heidelberg, Germany. * To whom correspondence should be addressed*

SUMMARY

The existence of both linear and radial non-steady state drug diffusion within rotationally-symmetric matrices and membranes held in a diffusion cell has been investigated. The error involved in the calculation of diffusivities from experimental release and permeation data using solutions to the linear form of Fick's Second Law could thereby be determined as a function of system geometry. For the case of drug release from a matrix, the use of a linear model underestimates the diffusivity, even for thin matrices (radius : height = 200). For drug permeation through a membrane, diffusivity will be overestimated with a linear model, the error also being strongly dependent on the value for partition coefficient.

I. INTRODUCTION

The release of a drug from a rectangular matrix or its permeation through a plane membrane are two common diffusional problems of great importance in the field of controlled release. The kinetics of either process can be investigated experimentally by using a diffusion cell. Although numerous designs are available for such cells,[1] they have in common the manner in which the matrix or membrane is affixed within the cell. As illustrated schematically in Figure 1a, the matrix or membrane is held taught

0957-7548/91/2/045-064@$2.00+0.10PP

within the cell, between either a backing plate for a matrix or a donor chamber for a membrane, and an acceptor chamber. The results of such experiments are expressed as release or permeation profiles of drug mass in the acceptor medium, $m_a(t)$, *versus* time, t. The diffusivity of the drug within either matrix, D_m, or membrane, D_s, can be calculated from a profile by using the appropriate solution to Fick's Second Law. If the drug is initially homogeneously distributed within the matrix or donor solution and membrane, the simplification is made that only linear diffusion of drug in the x-dimension occurs. The two diffusional models illustrated in Figure 1b can then be employed, for which analytical solutions to the linear form of Fick's Second Law for both sink[2a,3] and non-sink[2b,4] boundary conditions are known.

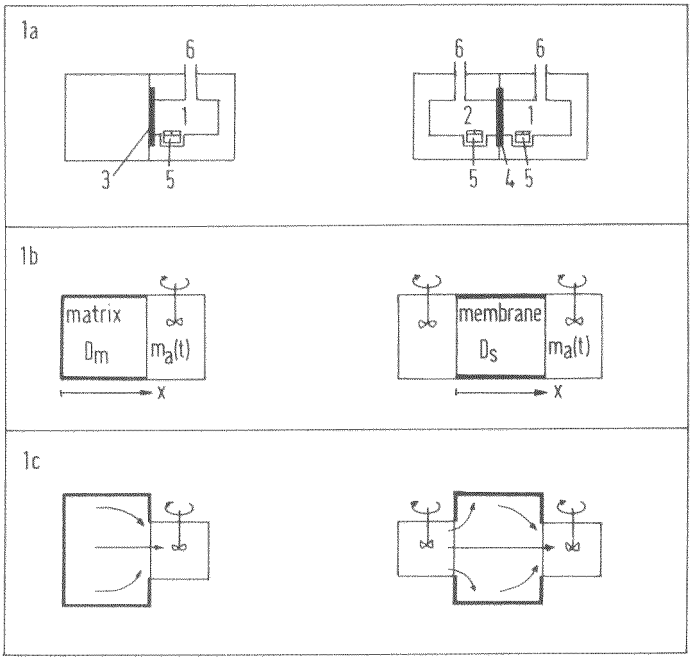

Figure 1. Schematic illustrations of drug release from a matrix (left) and drug permeation through a membrane (right). *a) Cross sections through a diffusion cell (1, acceptor chamber; 2, donor chamber; 3, matrix; 4, membrane; 5, stirrer; 6, sampling port). b) Linear diffusional models for the two processes (x, space coordinate; D_m, drug diffusivity in matrix; D_s, drug diffusivity in membrane; $m_a(t)$, drug mass in acceptor medium. c) Illustration of radial and linear drug diffusion within matrix and membrane.*

As part of a study of the transdermal application of the drug clenbuterol, we wished to make measurements of drug release and permeation using matrices and membranes of substantial thickness (up to 4 mm). A closer examination of

the geometry of the diffusion cell shows that in these cases the assumption of linear diffusion may be far from exact. Thus, Figure 1a shows how the matrix or membrane is larger in size than the area available within the cell for release or permeation. The edge region of the matrix or membrane necessary for fixation within the cell is not in contact with the opening of the donor or acceptor chambers. A true representation of the two models is given in Figure 1c for radially-symmetric bodies. It is clear that not only linear diffusion in the x-dimension occurs. Within the matrix, radial diffusion out of the edge region into its centre also takes place. Within the membrane, radial diffusion into the edge region occurs adjacent to the donor, and out of the edge region adjacent to the acceptor. The existence of both linear and radial diffusion within thick matrices or membranes is not taken into account by the linear models of Figure 1b. The use of solutions to the linear form of Fick's Second Law to calculate diffusivities from release or permeation data must, therefore, be subject to an error. The error arising in steady state flux has been shown some years ago by Barrer[5] to be negligible for permeation through very thin membranes. His steady state analysis does not, however, consider the error in calculated diffusivity, nor does it take into account the influence of partitioning. Additionally, it is uncertain at what matrix or membrane thickness the errors becomes large enough that they can no longer be ignored.

We have conducted an examination of the influence of matrix and membrane geometry on the size of the error. A numerical solution to a multi-dimensional form of Fick's Second Law for non-sink diffusion through matrices and membranes held in a diffusion cell is first derived. With the help of this model it is possible to predict the influence of system geometry on experimental release and permeation data. It is also used to evaluate results obtained from two series of experiments, namely, drug release from a thin polyacrylate matrix and drug permeation through a thick silicone membrane. The contrast between thick and thin bodies can thus clearly be made. Additionally, multi-dimensional diffusion can be made visible to the eye by examining the uptake of a dyestuff into a gel-matrix using digital image processing.

II. THEORY

The most general formulation of the problem to be solved is that of the non-steady state diffusion of dissolved drug with a single diffusivity, D, through the isotropic cylinder of finite length illustrated in Figure 2. The selection of suitable initial and non-sink boundary conditions allows the representation of either a matrix or a membrane held perpendicularly within a diffusion cell. Solution of this non-steady state problem is very involved. For the related case under sink boundary conditions, a formidable analytical solution is available.[6] The non-sink problem is, however, too ponderous to

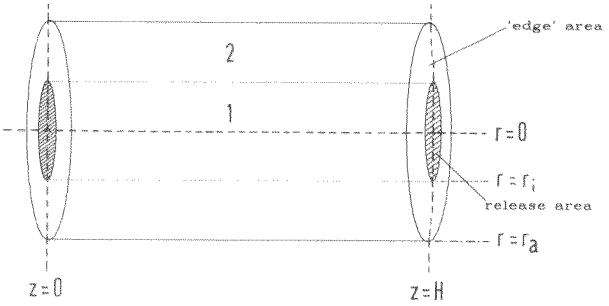

Figure 2. Geometric model applicable to non-steady state diffusion within a composite cylinder. *(1, inner layer of cylinder; 2, outer layer of cylinder; H, length of cylinder; r_a, total radius; r_i, radius of inner layer).*

be considered analytically, and must be tackled using numerical techniques. We solved the problem using Crank and Nicolson's implicit finite-difference method.[7,8] As the system is radially symmetric about the axis r=0 (see Figure 2), the drug concentration within the cylinder, c(r,z,t), is independent of angle, θ, and can be represented by the applicable form of Fick's Second Law[2c]:

$$\frac{\partial c(r,z,t)}{\partial t} = \frac{1}{r}\left[\frac{\partial}{\partial r}\left(rD\,\frac{\partial c(r,z,t)}{\partial r}\right) + \frac{\partial}{\partial z}\left(rD\,\frac{\partial c(r,z,t)}{\partial z}\right)\right] \quad , \; t>0 \ldots . (1)$$

The outer circumference of the cylinder represents the edge region and is insulated:

$$\frac{\partial c(r_a,z,t)}{\partial r} = 0 \qquad t>0 \qquad \ldots . (2)$$

For the case of release from a matrix, the cylinder can be represented by the finite difference grid illustrated in Figure 3a. By rotating the grid around its symmetry axis, the resulting body has the form of a cylindrical matrix. The grid points describe circles around the axis and delineate the points where the same drug concentration exists. Only those points marked with a cross lie within the release area of the face of the matrix, which is limited by an inner radius r_i. r_a is the total radius of the matrix. The drug is initially homogeneously dispersed within the matrix:

$$c(r,z,0) = c_o, \qquad 0 \le z \le H, \; 0 \le r \le r_a \qquad \ldots . (3)$$

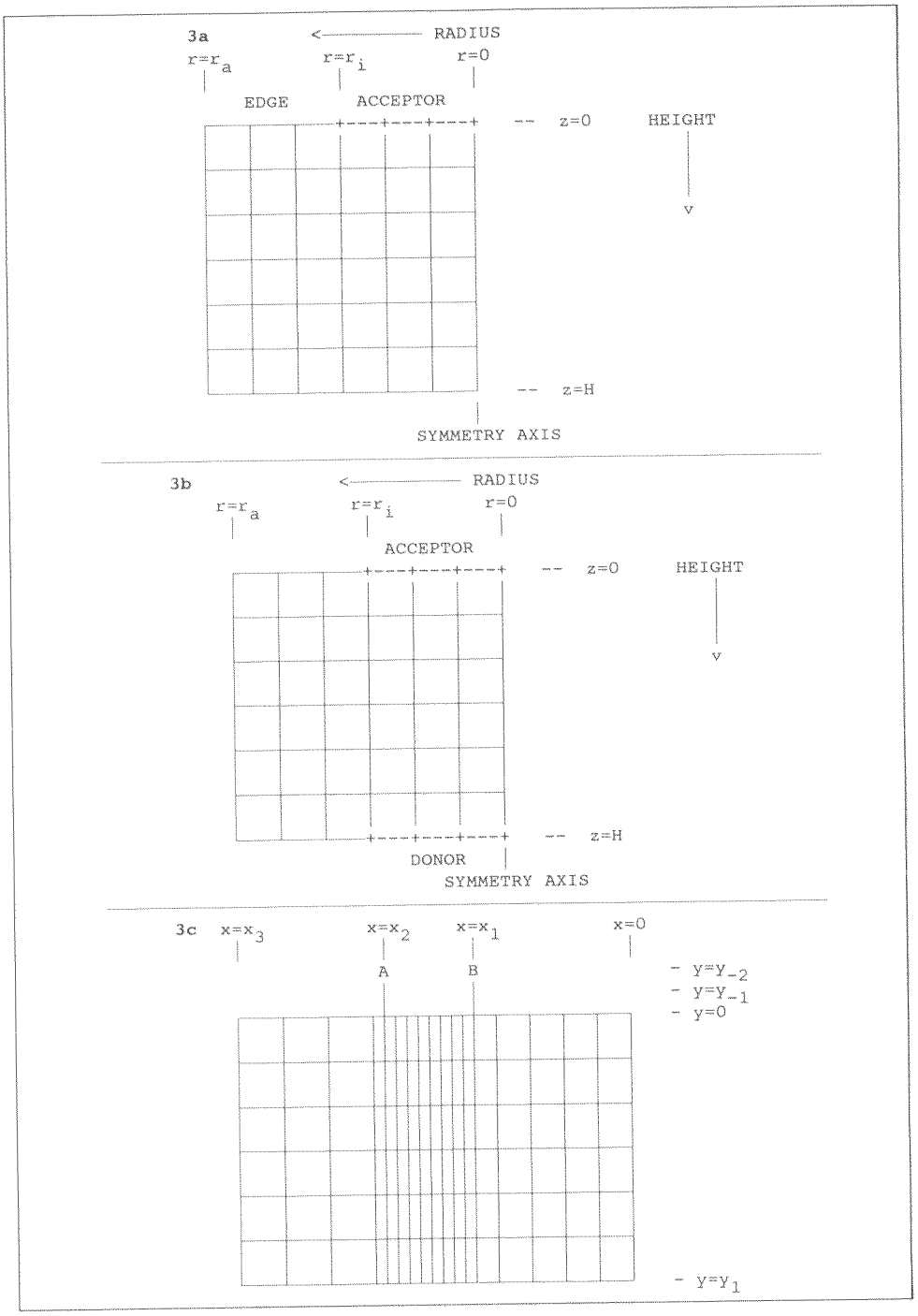

Figure 3. Finite difference grids. *a) Drug release from a matrix. b) Drug permeation through a membrane. c) Uptake into a gel-matrix.*

The whole area of the face at z = H is insulated:

$$\frac{\partial c(r,H,t)}{\partial z} = 0, \qquad 0 \le r \le r_a \qquad .....(4)$$

Drug release into a non-sink occurs through the inner layer (crosses) of the face at z = 0, the outer layer representing the edge region and being, therefore, insulated:

$$\frac{\partial c(r,0,t)}{\partial z} = 0, \; r_i \le r \le r_a; \qquad \frac{dm_a(t)}{dt} = -D_m \frac{\partial c(r,0,t)}{\partial z}, \; 0 \le r \le r_i \qquad ....(5)$$

$$K\, c_a(t) = c(r,0,t), \qquad 0 \le r \le r_i \qquad ....(6)$$

where K is the drug's partition coefficient between matrix and acceptor medium.

For the case of permeation through a membrane, the finite difference grid shown in Figure 3b is used. At z = H uptake of drug from the donor into the membrane occurs at the points marked with a cross ($z = H, 0 \le r \le r_i$). The complete model is described by rotating the grid around the symmetry axis. The drug is initially contained within a perfectly-stirred medium adjacent to the membrane's face at z = 0, the membrane being drug free:

$$c_d(0) = c_o; \quad c(r,z,0) = 0, \quad 0 \le z \le H, \; 0 \le r \le r_a \qquad ....(7)$$

Uptake of drug from the donor medium occurs through the inner layer (crosses) of the face at z = H, with the outer layer representing the edge region and being insulated:

$$\frac{\partial c(r,H,t)}{\partial z} = 0, \quad r_i \le r \le r_a; \qquad \frac{dm_d(t)}{dt} = -D_s \frac{\partial c(r,H,t)}{\partial z}, \; 0 \le r \le r_i \qquad ....(8)$$

$$K\, c_a(t) = c(r,0,t), \qquad 0 \le r \le r_i \qquad ....(9)$$

where K is the drug's partition coefficient between membrane and donor/acceptor medium. The non-sink release of drug through the inner layer (crosses) of the face at z = 0 is described, as for the matrix, by Equations 5 and 6.

III. MATERIALS AND METHODS

3.1 Solution of models and simulation of theoretical behaviour

The finite difference representations of the initial and boundary conditions were first derived. For drug release from a matrix, the resulting forms of Equations 1-6 form a linear system of multi-diagonal matrices that was programmed in Pascal on an Epson PC (80 386 processor with 80 387 coprocessor). For drug permeation through a membrane, the finite difference forms of Equations 1, 2 and 5-9 were similarly programmed. Solution by Gauss's elimination method yielded both the theoretical drug concentration profile within matrix or membrane, c(r,z,t), and the theoretical release or permeation profile, $m_a(t)$.

3.2 Measurement of drug release from a thin polyacrylate matrix

The model was used to evaluate some results obtained for the release of the basic drug clenbuterol (MWt = 277, pK_a = 9.5; Boehringer Ingelheim, Germany) from matrices prepared from purified[9] Eudragit NE30D (Röhm Pharma, Darmstadt, Germany). The 50 μm-thick matrices were prepared by solvent casting.[10] The release rate into pH 8 phosphate buffer was undertaken using the glass diffusional cell illustrated schematically in Figure 1a and operated as described before.[11] Two solutions to Fick's Second Law were then fitted to the experimentally-determined release profile, $m_a(t)_{exp}$: the numerical solution for the linear release model[11] illustrated in Figure 1b; and the numerical solution to the multi-dimensional release model illustrated in Figures 2 and 3a. An improved simplex method was used for the fit[12], which yielded the best value for D_m.

3.3 Measurement of drug permeation through a thick silicone membrane

An evaluation of the experimental permeation of clenbuterol through a thick poly(dimethyl)siloxane membrane was also undertaken with the model. The membrane was prepared by vulcanising dimethyl dichlorosilane with 3% Hardner T (Wacker Chemie, Munich, Germany) at 70°C for 12 h in a 4 mm deep, circular teflon mold. The diffusional cell illustrated in Figure 1a was used as described before[11], with Miglyol 840 (Dynamit Nobel, Witten, Germany) as a donor and acceptor medium to ensure high drug solubility. The linear[11] (Figure 1b) and multi-dimensional (Figure 3b) models were then fitted to the experimentally-determined permeation profile, $m_a(t)_{exp}$, yielding the best values in this case for both D_s and K.

3.4 Measurement of uptake into a thick agarose gel matrix

With this experiment, the edge effect could be made visible to the naked eye. A plexiglas diffusion cell was used, which had a geometry equivalent to that of matrix and acceptor illustrated in Figure 1c. It allowed examination of the two-dimensional uptake of a dyestuff from a donor medium into a solid gel. The gel was prepared from a 5% seaplaque agarose sol (FMC Corporation, Rockland, USA) that had been allowed to set within the diffusion cell. 2 ml of a 1% w/w aqueous methylene blue (Merck, Darmstadt, Germany) solution were then carefully filled into the neck of the cell at room temperature. The dyestuff diffused into the gel to produce a visible, two-dimensional profile of blue colour-intensity. Digitalized photographs of the cell were taken at regular intervals up to 56 h with a ccd camera (WVCD 110E, Panasonic, Tokyo, Japan) connected to a IBM-AT containing an 8 bit digitial image processing card (MVP-AT, Matrox Ltd., Canada). A resolution of 512 x 512 picture points with shades on a scale of 0 to 255 was used, the latter being subsequently converted into concentration profiles, c(r,z,t), with the help of calibration gels of known dyestuff concentration.

To calculate diffusivity, the applicable multi-dimensional numerical solution to Fick's Second Law was fitted to each concentration profile. A complication arose here in the design of a two-dimensional finite difference grid to fit the contours of the diffusion cell. For a constant step size in space, delta x, the edge points A and B at the neck of the cell and also the side walls of the cell did not necessarily coincide with grid points. To account for this, the grid was deformed as illustrated in Figure 3c. Delta x is now not constant across the grid from $x = 0$ to $x = x_3$. The isolated grid points A and B take into account the concave shape of the gel surface. The origin of the coordinate system is the upper right corner of the cell at the point (0|0). Problems arise at those grid points where delta x changes. At a specific grid point (e.g. $x_1|0$), the two neighbouring points on the x axis are now not equally distanced. The usual finite difference form of Equation 1 (i.e. the Crank-Nicolson formula) cannot be applied at that point. A solution to this problem was taken from Crank[2d] by using a Lagrange interpolation. The resulting set of equations was solved by an improved Gauss algorithm to step over zero elements. As before, the fit of this theoretical solution to the experimental c(z,r,t) values yielded the best values for D and K.

IV. RESULTS AND DISCUSSION

4.1 Drug release from a matrix

Fig 4a shows the theoretical concentration-distance profile within a cylindrical thick matrix whose radius equals its height (i.e. r:h = 1). The

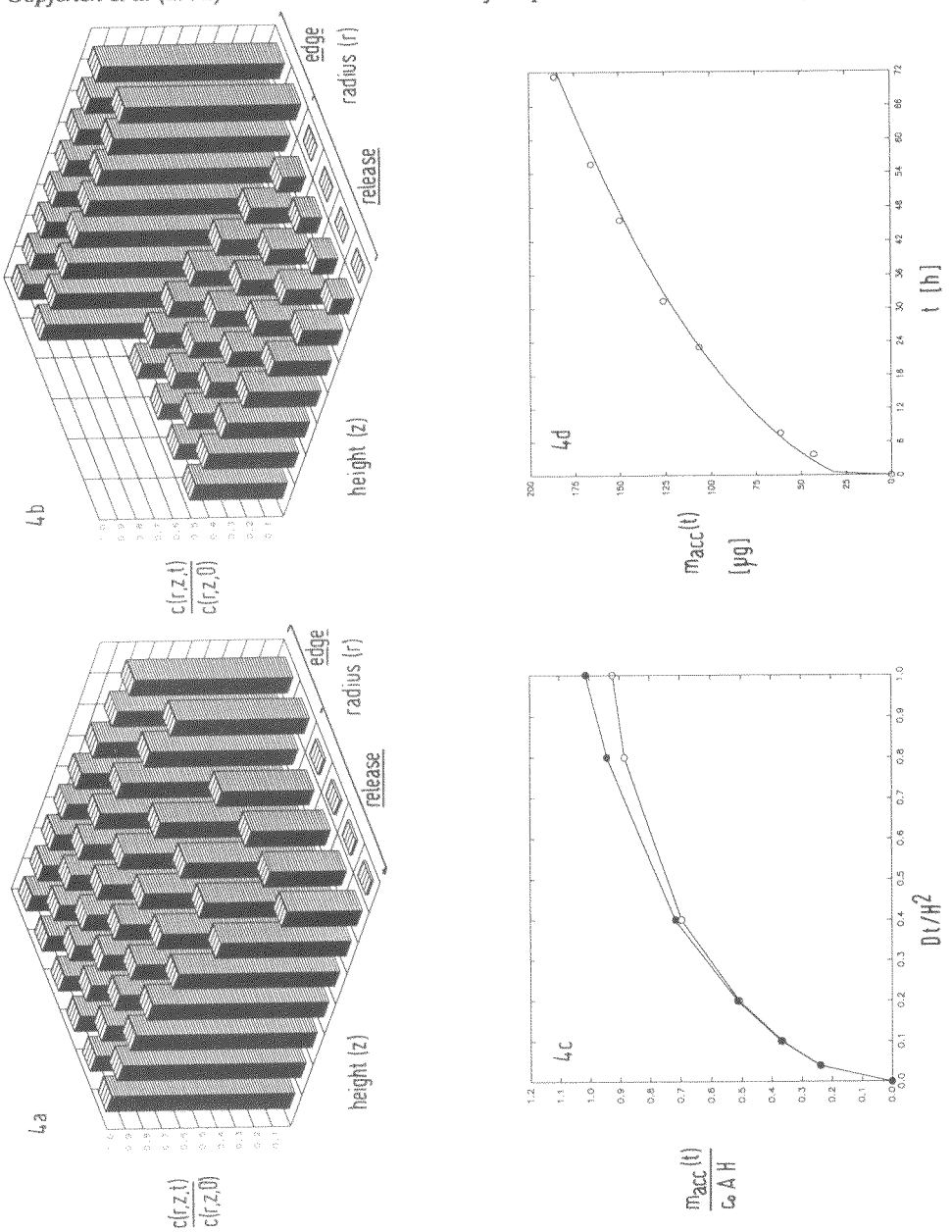

Figure 4. Drug release from a cylindrically-shaped matrix. *a) Theoretical concentration-distance profile within a thick matrix (r:h = 1; $D_m t / H^2$ = 0.04; K = 1). b) Theoretical concentration-distance profile within a thin matrix (r:h = 10; $D_m t / H^2$ = 0.04; K = 1). c) Theoretical release profiles from a thin matrix (r:h = 10) for linear (o) and multi-dimensional (●) diffusion. d) Typical experimental release profile (coordinates) for clenbuterol from purified Eudragit N30D-matrix (8% w/w drug loading) together with curve of best fit to multi-dimensional model.*

vertical axis denotes the drug concentration relative to its initial value, c(r,z,t)/c(r,z,0), and the x/y plane defines the axis or height of the matrix and its radius. As the diffusion problem is rotationally symmetric, this representation is sufficient to describe the drug concentration profile within the whole matrix. The profile is determined by the grid in Figure 3a and is represented by 8 numerical grid points along the height and 6 along the radius. The latter are further divided in 4 grid points lying within the area of release, and 2 grid points representing the edge area of the matrix by which it is held within the diffusion cell. There is a marked concentration gradient along the cylinder axis, which is that taken into account with the linear model of Figure 1b. The concentration also decreases, however, in the radial direction adjacent to the acceptor, from the outermost point of the radius (i.e. in the edge) towards the centre of the matrix. This illustrates the existence of a mass flux out of the edge area that is not considered when evaluating experimental data with the linear model. The magnitude of this flux out of the edge is diminished for a thiner matrix where the ratio r:h is, say, 10 (Figure 4b). The edge region is now depleted less, owing to the longer diffusional pathway existing along the extended radial axis compared with the short pathway along the height.

TABLE 1

FITTED DIFFUSIVITIES (D) FOR CLENBUTEROL RELEASE FROM A PURIFIED EUDRAGIT NE30D-MATRIX (r:h = 200) OBTAINED FROM LINEAR (1D) AND MULTI-DIMENSIONAL (3D) MODELS

drug loading	n	D x 10^{11} [cm^2/s]
6 %	4	1D* 0.58 ± 0.087 3D 0.56 ± 0.074
8 %	4	1D* 0.93 ± 0.071 3D 0.91 ± 0.071
10 %	4	1D* 1.57 ± 0.091 3D 1.53 ± 0.103
12 %	4	1D* 2.81 ± 0.427 3D 2.76 ± 0.426
16 %	4	1D* 3.70 ± 0.30 3D 3.44 ± 0.286
20 %	4	1D* 2.36 ± 0.522 3D 1.80 ± 0.413

* taken from ref 9.

The theoretical release profile in the acceptor, $m_a(t)$, strongly depends on the relative size of the release area available. If the complete area is available for release (i.e. no edge exists), then a linear model is exact, whereas a reduction in the release area due to the existence of an edge necessitates application of the multi-dimensional model. Figure 4c shows how the two theoretical release profiles differ for r:h = 10, the amount of dug released being greater if the existence of the edge is recognised. Fitting of the release profile for multi-dimensional release to a linear model must, therefore, lead to erroneous values for diffusivity. The diffusivity determined will be larger than its true value, as the release profile for the linear release process is always lower than that for the three-dimensional one.

An example of experimental release coordinates, $m_a(t)_{exp}$, for clenbuterol from the purified Eudragit NE30D-matrix is shown in Figure 4d, together with the curve of best fit to the multi-dimensional model. The fit appears visually good. Table 1 compares the values for diffusivity obtained from this fit with those obtained from a fit to the linear model. The differences are small in this case, since a thin matrix was used for the experiment (r:h = 200). The conclusion drawn from Figure 4c is, however, confirmed experimentally, that a high diffusivity is obtained when evaluating data with a linear model. The apparent concentration dependence of the diffusivity seen here has been noted before.[9,11]

4.2 Drug permeation through a membrane

An example of a theoretical concentration-distance profile within a thick (r:h = 1) cylindrical membrane is given in Figure 5a for short times. The drug is taken up from the donor into the membrane at z = H and released into the acceptor at z = 0. The drug concentration at z = H increases at all grid points, including those of the edge which have no direct contact with the donor, illustrating clearly the edge effect. The drug concentration at the grid points lying in direct contact with the donor are the largest seen and are all equal as a result of Equation 9. The concentration decreases in a curvelinear fashion within the membrane in the direction towards the acceptor. With advancing time a pseudo-steady state is reached (Figure 5b), as designated by the establishment of an almost linear concentration-distance profile from the donor towards the acceptor.

Theoretical mass-time profiles in the acceptor are shown in Figure 5c for both linear and multi-dimensional diffusion. The profile for linear diffusion is higher at short times, whereas the subsequent pseudo-steady state flux is higher for the multi-dimensional case. The edge surrounding the diffusional area in contact with the donor takes up a part of the diffusing drug at early times (*cf.* Figure 5a). Fewer molecules will, therefore, diffuse directly through the membrane and arrive in the acceptor, extending the lag

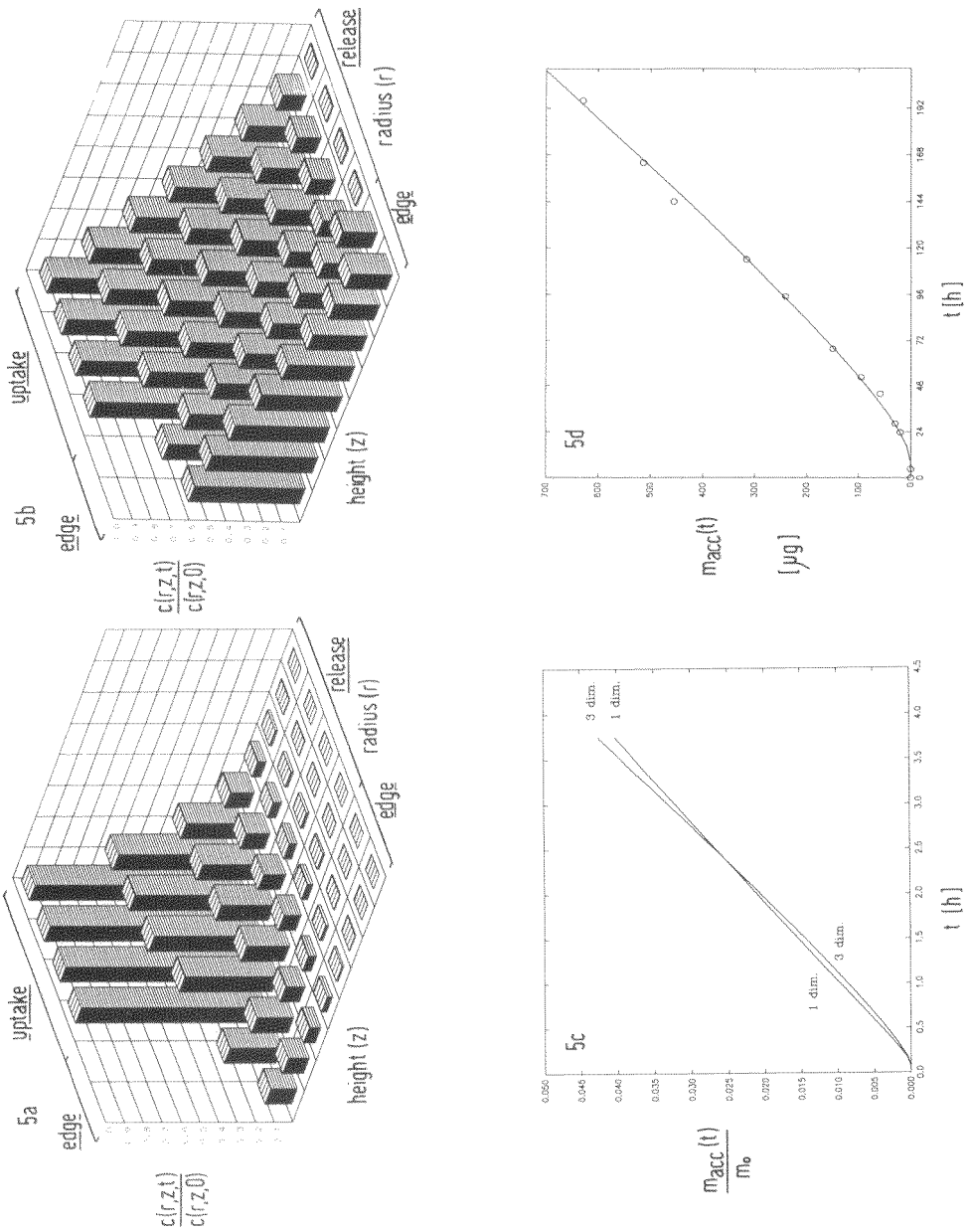

Figure 5. Drug permeation through a cylindrically-shaped membrane. *a) Theoretical concentration-distance profile within a thick membrane (r:h = 1; $D_m t / H^2 = 0.04$; K = 1) for short time. b) Theoretical concentration-distance profile within a thick membrane (r:h = 1; $D_m t / H^2 = 0.4$; K = 1). c) Theoretical permeation profiles through thick (r:h = 1) membrane for linear and multi-dimensional diffusion. d) Typical experimental permeation profile (coordinates) for clenbuterol through thick (r:h = 0.42) silicone membrane together with curve of best fit to multi-dimensional model.*

time. Indeed, the two curves in Figure 5c show different lag-times; that for the curve resulting from 3-dimensional diffusion is twice as long. Once the lag-phase is past, the edge of the membrane now provides a source of additional drug to the release area. The grid point lying in contact with the acceptor and directly adjacent to r_i (*cf.* Figure 3b) receives drug from three neighbours, instead of only one in the case of a linear model. This increases the flux of drug out of the membrane into the acceptor at later times (*cf.* Figure 5b). When evaluating experimental permeation data using a linear model, the longer lag-time arising from multi-dimensional diffusion will lead to an underestimation in diffusivity. This is the opposite effect to that seen with drug release from a matrix (*cf.* Figure 4c) and can be confirmed from the experimental permeation results obtained here. Thus, Figure 5d shows an example of the coordinates of $m_a(t)_{exp}$ for clenbuterol permeation through the thick polysiloxane membrane (r:h = 0.42), together with the best-fitting solution to the multi-dimensional model. The values from this fit for diffusivity, partition coefficient, and pseudo-steady state flux (Table 2) differ to those obtained from a fit to the linear model. Diffusivity is indeed smaller for the linear model and flux greater, as predicted from Figure 5c.

TABLE 2

FITTED DIFFUSIVITIES (D), PARTITION COEFFICIENTS (K), AND FLUXES (J) FOR CLENBUTEROL PERMEATION THROUGH A THICK SILICONE MEMBRANE (r:h = 0.42) OBTAINED FROM LINEAR (1D) AND MULTI-DIMENSIONAL (3D) MODELS

model	n	D $x10^7$ [cm^2/s]	K	J [$\mu g*cm^{-2}*s^{-1}$]
1D	3	2.496 ± 0.117	0.168 ± 0.019	3.611 ± 0.082
3D	3	3.245 ± 0.349	0.136 ± 0.022	4.058 ± 0.114

The magnitude of the error in measured diffusivity and flux can be related to the geometry of the membrane. The latter can conveniently be defined by two factors based on the geometry shown in Figure 2. The first relates the area of the edge region not in direct contact with donor or acceptor to the total area of the matrix or membrane: $100\ (r_a - r_i)/r_i$; and the second the thickness of the matrix or membrane, H, to its total radius, r_a: $100\ H/r_a$. The values for the theoretical pseudo-steady state flux and the

lag-time were determined from simulated multi-dimension permeation profiles, and the %-deviation from a linear simulation calculated. Figure 6a shows the %-deviation in flux from the value without edge effect, $100x(J_{3D}-J_{1D})/J_{1D}$, as a function of increasing outer radius (i.e. greater edge area), $100x(r_a-r_i)/r_i$, for increasing ratios of H/r_a and a partition coefficient of 0.1. The deviations vary between -5 and 30%. The shape of these curves is determined by two effects. With an increase in outer radius, r_a, the flux initially increases owing to the additional diffusional flux from the edge region (*cf.* Figure 5b). This finding is in agreement with Barrer's previous analysis under steady state conditions.[5] Further increase in r_a then decreases the flux, an effect not seen with the steady state analysis. This is caused by the increasing volume of the matrix, which leads to greater amounts of drug being retained within the membrane under non-sink conditions. Since only a finite amount of drug is present within the system, the concentration gradient is lowered, and the flux decreases. The differences seen between the 'thick' ($H/r_a=1$) and 'thin' membranes ($H/r_a=0.25$) in Figure 6a shows how the latter are less liable to error when evaluating permeation data with a linear model, in agreement with Barrer's steady state analysis.[5] Increasing the partition coefficient to K=1 (Figure 6b) increases the amount of drug retained within the membrane. As a result, the curves fall off earlier than those in the Figure 6a. By raising the partition coefficient further to K=10 (Figure 6c), the depression of the flux is even stronger, so that the curves decrease from the origin.

The deviations in the lag-time for K = 0.1 are shown in Figure 7a. As with the flux, there are two discernible effects. With increasing outer radius of the membrane, r_a, uptake of drug within the edge area leads to longer lag-times. A subsequent decrease is, however, again caused by the increasing volume of the membrane. This leads to a faster decrease in the donor concentration, with the curves reaching their point of inflexion earlier. The time-lag is thereby shortened, with deviations of up to 250% occuring. This partitioning effect which depresses the lag-time at high membrane volumes is again more pronounced when the partition coefficient is increased to K = 1 (Figure 7b). The curves fall off earlier, and the deviations in the lag-time are smaller. With a further increase in the partition coefficient to K = 10 (Figure 7c), the curves fall off even earlier, and the deviations are further diminished.

Figures 6 and 7 can be regarded as error nomograms, which give the errors in flux and lag-time (and hence diffusivity) arising from the evaluation of permeation data with a linear model. For known diffusion cell geometry and values of r:h, the errors to be expected can be directly read off. The strong influence of the partition coefficient clearly cannot be disregarded.

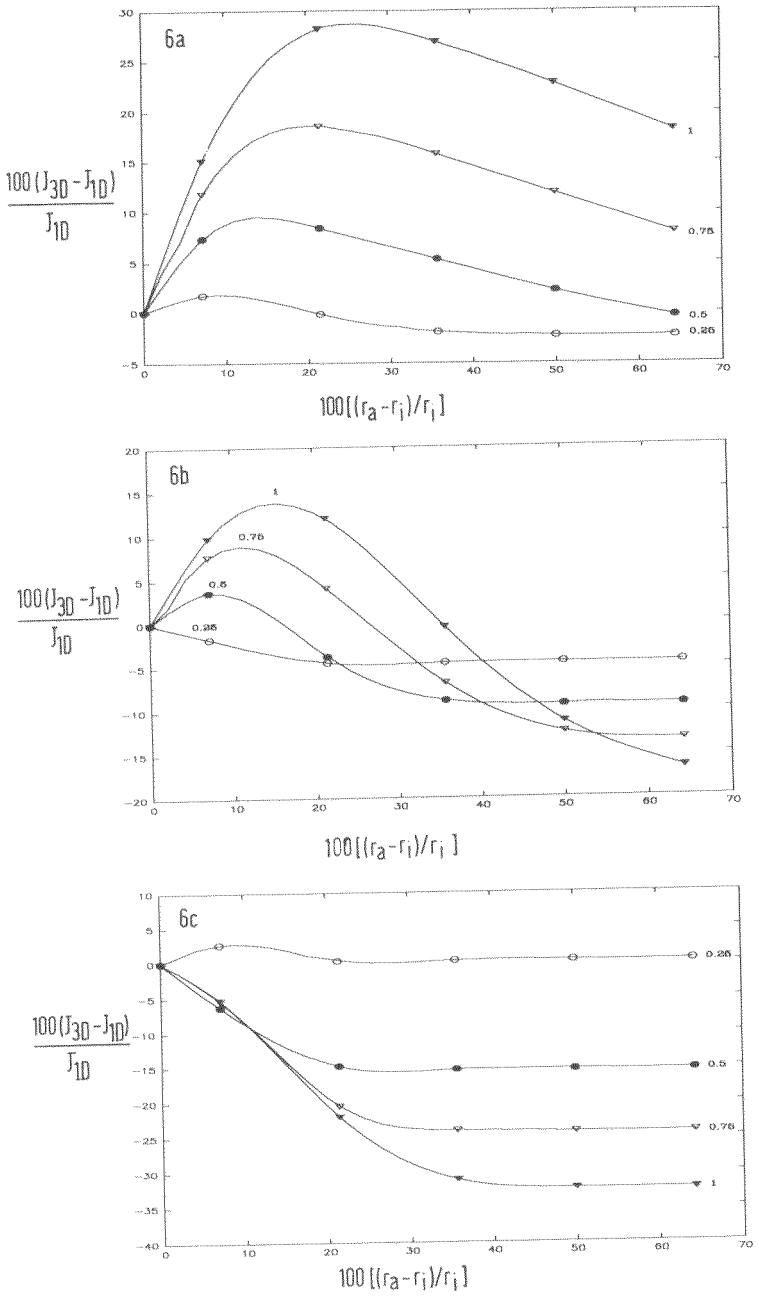

Figure 6. Error nomograms for deviation in flux from value without edge effect [100 x $(J_{3D}-J_{1D})/J_{1D}$] as a function of increasing outer radius [100 x $(r_a-r_i)/r_a$)] for increasing ratios of H/r_a. *(a, K = 0.1; b, K = 1; c, K = 10).*

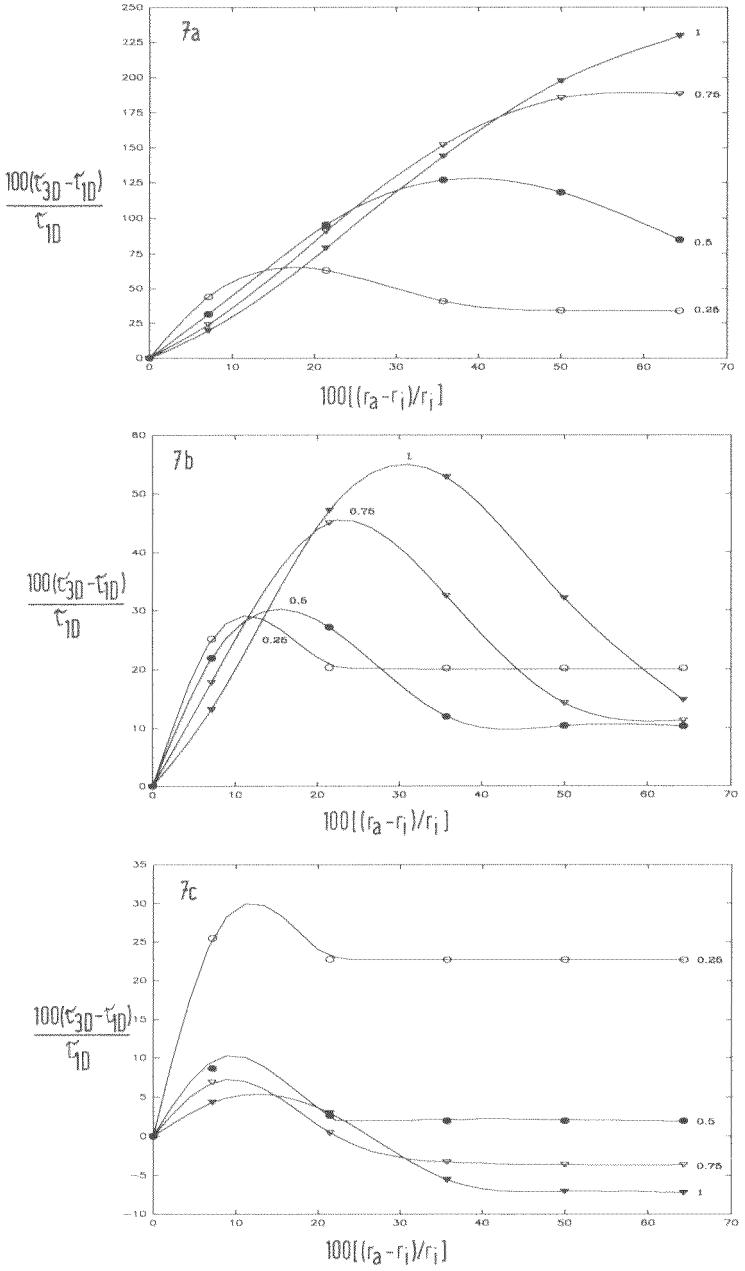

Figure 7. Error nomograms for deviation in lag-time from value without edge effect [100 x $(\tau_{3D}-\tau_{1D})/\tau_{1D}$] as a function of increasing outer radius [100 x $(r_a-r_i)/r_a$] for increasing ratios of H / r_a. *(a, K = 0.1; b, K = 1; c, K = 10).*

4.3 Uptake into a thick agarose gel matrix

A theoretical concentration-distance profile within the gel after short time is shown in Figure 8a. The symmetric cell yields a profile symmetric to the symmetry axis of the grid. At this early time, the diffusant reaches but few of the grid points not directly adjacent to the donor. The concentration in the edge area is also increasing, illustrating the existence of multi-dimensional diffusion. Figure 8a also shows how at a later time (italics), the diffusant extends throughout almost the whole cell. Apart from the concentration gradient existing along the vertical axis of the gel that arises from linear diffusion, a concentration gradient along the horizontal axis can also clearly be seen. This demonstrates the existence of both linear and radial diffusion within the gel. The decreasing concentration at the donor/gel interface reflects the non-sink boundary condition prevailing there.

The existence of multi-dimensional diffusion can be seen nicely in Figure 8c, where a time-series of digitalized photographs taken of the cell during the experiment with methylene blue is shown. The dye diffuses linearly and radially into the gel, with the edge area also taking up dyestuff. The curvature of the dyestuff front arises from the concave shape of the gel surface. The concentration profile within the gel calculated from these digitalized pictures by picture processing for the example of 7.72 h is shown in Figure 8b. Those values at the grid points in the centre of the cell were fitted to the multi-dimensional model in Figure 3c to yield the theoretical profile shown in italics in the same figure. The theoretical and experimental values are in good agreement with one another, a Chi^2 test showing that there is no difference between both curves ($\alpha = 0.05$). A fitted diffusivity of $3.35 \times 10^{-6} \pm 0.18 \times 10^{-6}$ $cm^2 s^{-1}$ was obtained, together with a fitted partition coefficient of 1.18 ± 0.2 ($n = 3$). Digital picture processing thus represents a simple and exact method for determining diffusivity (and partition coefficient) within solid bodies. The diffusant must be coloured, although fluorescent marked substances could also be used. The calculation can be made simpler by measuring linear diffusion within a long glass capillary, allowing use of the applicable analytical solution to Fick's Second Law.

V. ACKNOWLEDGEMENTS

We thank Boehringer Ingelheim KG for its support of this project. A part of the work was presented by AG in March 1990 at the 32nd Scientific Meeting of the Arbeitsgemeinschaft für Pharmazeutische Verfahrenstechik (APV) in Kiel, Germany.

8a

		85.73	DONOR		85.73		
		74.45			*74.45*		
	EDGE AREA					EDGE AREA	
0.000	0.004	2.218	85.73	85.73	2.218	0.004	0.000
0.485	*3.884*	*44.03*	*74.45*	*74.45*	*44.03*	*3.884*	*0.485*
0.000	0.000	0.016	0.984	0.884	0.016	0.000	0.000
0.207	*1.511*	*13.64*	*25.88*	*25.88*	*13.64*	*1.511*	*0.207*
0.000	0.000	0.000	0.006	0.006	0.000	0.000	0.000
0.051	*0.353*	*2.969*	*6.123*	*6.123*	*2.969*	*0.353*	*0.051*
0.000	0.000	0.000	0.000	0.000	0.000	0.000	0.000
0.009	*0.060*	*0.491*	*1.076*	*1.076*	*0.491*	*0.060*	*0.009*
0.000	0.000	0.000	0.000	0.000	0.000	0.000	0.000
0.001	*0.008*	*0.065*	*0.149*	*0.149*	*0.065*	*0.008*	*0.001*
0.000	0.000	0.000	0.000	0.000	0.000	0.000	0.000
0.000	*0.001*	*0.007*	*0.017*	*0.017*	*0.007*	*0.001*	*0.000*
0.000	0.000	0.000	0.000	0.000	0.000	0.000	0.000
0.000	*0.000*	*0.001*	*0.002*	*0.002*	*0.001*	*0.000*	*0.000*
0.000	0.000	0.000	0.000	0.000	0.000	0.000	0.000
0.000	*0.000*	*0.000*	*0.000*	*0.000*	*0.000*	*0.000*	*0.000*

8b

			donor				
	edge area					edge area	
18.9	32.1	46.3	72.9	69.3	47.3	40.5	19.3
22.2	*35.9*	*46.2*	*56.1*	*56.8*	*48.9*	*44.3*	*25.1*
15.0	21.4	26.0	32.8	34.8	25.3	23.9	16.3
15.9	*24.1*	*29.3*	*35.2*	*35.7*	*30.9*	*28.7*	*17.8*
10.6	15.3	17.2	19.5	19.7	17.7	16.7	11.5
9.9	*14.3*	*17.0*	*20.2*	*20.5*	*17.9*	*16.8*	*11.0*
6.5	8.9	10.6	12.1	11.9	10.6	10.1	7.1
5.5	*7.8*	*9.1*	*10.7*	*10.9*	*9.6*	*9.1*	*6.1*
4.2	5.5	6.1	7.1	6.9	6.5	6.1	4.4
3.1	*4.2*	*4.9*	*5.8*	*5.8*	*5.2*	*4.9*	*3.4*

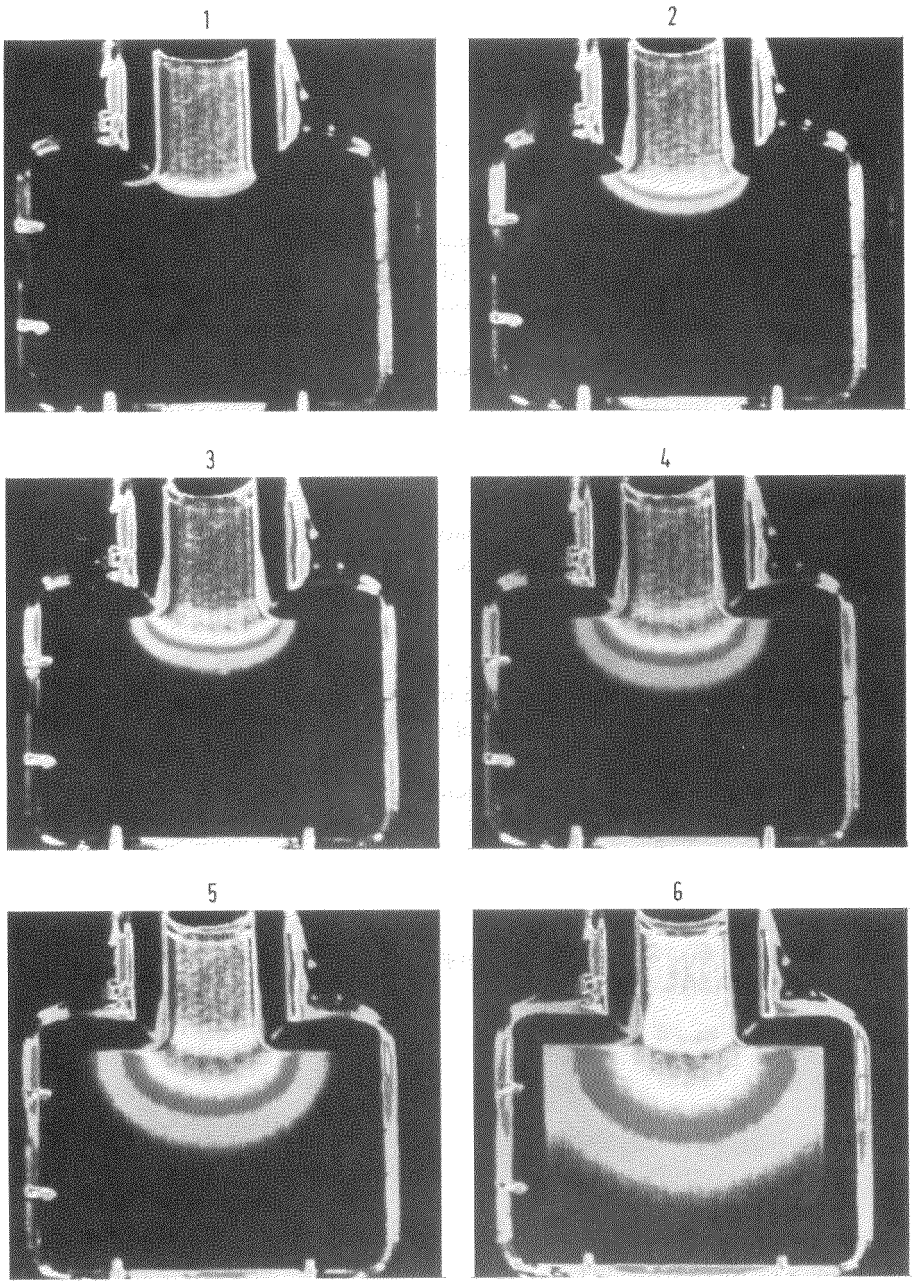

Figure 8. Uptake of methylene blue into agarose gel. *a) Theoretical concentration-distance profile within gel after short time ($D = 1 \times 10^{-6}$ cm^2 s^{-1}; t = 10,000 s) and long time (italics) ($D = 1 \times 10^{-6}$ cm^2 s^{-1}; t = 500,000 s). b) Experimental concentration-distance profile after 8 h together with profile of best fit to multi-dimensional model (italics). c) Sequence of digitalised pictures within agarose gel (1:0 h; 2:0.72 h; 3:1.73 h; 4:3.73 h; 5:7.72 h; 6:21.7 h.*

VI. REFERENCES

1. Tojo, K. (1987). Design and calibration of in vitro permeation apparatus. In: Chien, Y., ed., *Transdermal controlled systemic medications*, Marcel Dekker, New York, pp 127-158.
2. Crank, J. (1975). *The mathematics of diffusion*, 2nd Ed., Oxford University Press, London: a) pp 47-49; b) pp 56-59; c) p5; d) pp316-318.
3. Barrer, R.M. (1951). *Diffusion in and through solids*, Cambridge University Press, London, p 51.
4. Spacek, P. and Kubin, M. (1967). Diffusion in gels. *J. Poly. Sci.*, **C16**, 705-714.
5. Barrer, R.M., Barrie, J.A. and Rogers, M.G. (1963). Permeation through a membrane with mixed boundary conditions. *Trans. Farad. Soc.*, **58**, 2473-2483.
6. Ölcer, N.Y. (1968). A general class of unsteady heat flow problems in a finite composite cylinder. *Quart. Appl. Math.*, **26**, 355-371.
7. Crank, J. and Nicolson, P. (1947). A practical method for numerical evaluation of solutions of partial differential equations of the heat conduction type. *Proc. Camb. Phil. Soc.*, **43**, 50-67.
8. Smith, G. (1987). *Numerical solution of partial differential equations: finite difference methods*, 3rd Ed, Oxford University Press, London, pp 19-38.
9. Göpferich, A. and Lee, G. (1992). The influence of indiginous surfactant on the structure and drug-release properties of Eudragit NE30D-matrices. *J. Cont. Rel.*, submitted.
10. Zierenberg, B. (1985). Einsatz des Nelder-Mead-Verfahrens zur Optimierung der Freigabeparameter von Polymersystemen für Arzneistoffe. *Acta Pharm. Technol.*, **30**, 17-21.
11. Göpferich, A. and Lee, G. (1991). Measurement of drug diffusivity in stratum corneum membranes and a polyacrylate matrix. *Int. J. Pharm.*, in press.
12. Nelder, J. and Mead, R. (1967). A simplex method for function minimisation. *Computer J.*, **10**, 308-313.